

Through-space charge transfer and emission color tuning of di-*o*-carborane substituted benzene†Cite this: *Dalton Trans.*, 2014, **43**, 4978Hye Jin Bae,^a Hyungjun Kim,^a Kang Mun Lee,^a Taewon Kim,^b Yoon Sup Lee,^a Youngkyu Do*^a and Min Hyung Lee*^b

1,4-Di-(1-Ar-*o*-carborane-2-yl)benzene (Ar = 3,5-bis(trifluoromethyl)phenyl (**1**), phenyl (**2**), 4-*n*-butylphenyl (**3**), 4-*N,N*-dimethylaniline (**4**)) compounds that are electronically modulated at the C1-position of *o*-carborane with the electron-withdrawing or -donating aryl groups were prepared and characterized. The X-ray crystal structures of **1**, **3**, and **4** reveal that the two aryl groups on the C1-carborane carbon atoms are oppositely positioned, featuring overall C₂-symmetry, and the C1–C2 bond length of carborane increases with the increasing order of electron-donating effect of an aryl group. UV-vis absorption spectra exhibit small low-energy absorption bands at around 275–300 nm for **1–3** while **4** shows a broad absorption tail at 350–400 nm. Although **1–4** show virtually no emission in solution, an intense aggregation-induced emission over the region ranging from 400–700 nm is observed in the solid state. Importantly, the emission wavelengths of **1–4** exhibit an apparent red-shift upon changing the aryl substituent from the CF₃ to the NMe₂ group (from **1** to **4**). TD-DFT calculations suggest that the low-energy electronic transition is attributed to the intramolecular “through-space” charge transfer between the appended aryl group (HOMO) and the central phenylene ring (LUMO), and the greater change in the HOMO level by the substituent than that in the LUMO is responsible for the emission color tuning.

Received 7th September 2013,
Accepted 9th October 2013

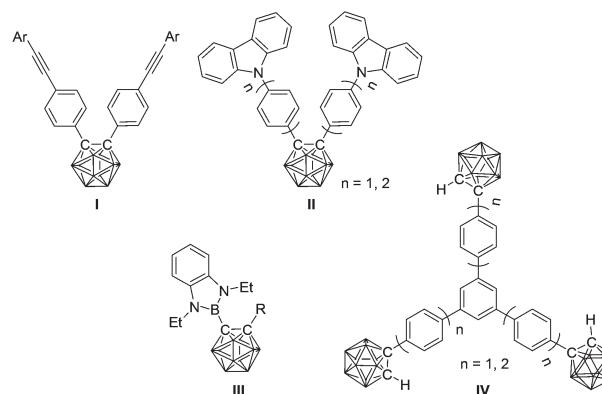
DOI: 10.1039/c3dt52465e

www.rsc.org/dalton

Introduction

ortho-Carborane (1,2-dicarba-*closo*-dodecarborane) has recently received attention in the field of luminescent materials for the potential optoelectronic applications of *o*-carborane derivatives.^{1–3} It has been shown that the emission properties of luminophores such as emission color and quantum efficiency are largely affected by the incorporation of *o*-carborane,^{1–14} probably owing to the unique properties of *o*-carborane such as highly polarizable σ -aromatic character and electron-withdrawing property through C-substitution.¹⁵ Recent reports on the photophysics of carborane-containing luminophores suggested that *o*-carborane is involved in the charge transfer (CT) transition and can alter the excited state properties of luminophores.^{5,7,9} For example, Chujo and co-workers have reported that CT-based aggregation-induced emission (AIE) can be activated in the various 1,2-diaryl-*o*-carborane compounds (**I**) and their emission color can be fine-

tuned by the substituent on an aryl group.⁹ The donor-acceptor dyads consisting of carbazole and *o*-carborane moieties have also been reported by Kang and co-workers (**II**).⁷ It was revealed that efficient photoinduced CT from a carbazole donor to a carborane acceptor forms a discrete charge-separated excited state. Fox and co-workers have reported CT transition in the diazaboroly-*o*-carborane donor-acceptor systems (**III**) and shown that the CT transition is affected by the substituent on the carborane and molecular geometry.⁵ Hosmane *et al.* have reported the luminescent properties of organic π -systems decorated by *o*-carborane moieties (**IV**).^{10,11}



The foregoing reports and our recent results^{1,3,4,13} on the carborane-containing luminophores suggest that *o*-carborane

^aDepartment of Chemistry, KAIST, Daejeon, 305-701, Republic of Korea. E-mail: ykdo@kaist.ac.kr; Fax: +82 42 350 2810; Tel: +82 42 350 2869

^bDepartment of Chemistry and EHSRC, University of Ulsan, Ulsan 680-749, Republic of Korea. E-mail: lmh74@ulsan.ac.kr; Fax: +82 52 259 2348; Tel: +82 52 259 2335

†Electronic supplementary information (ESI) available: Theoretical details. CCDC 943435 (for **1**), 943436 (for **3**), and 943437 (for **4**). For ESI and crystallographic data in CIF or other electronic format see DOI: 10.1039/c3dt52465e

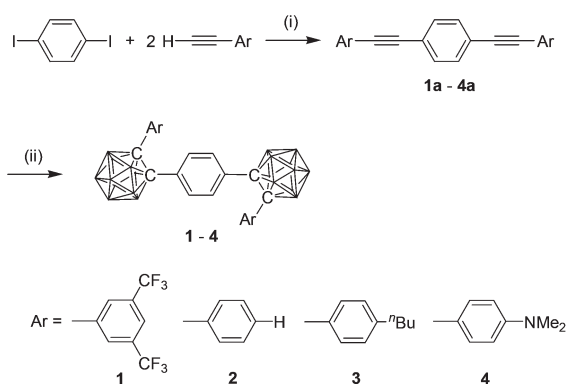
can directly participate in the lowest unoccupied molecular orbitals (LUMOs) of organic π -systems by the conjugation effect and thereby affecting the CT excited state. One of the consequences is weak or the non-emissive nature of the carborane-containing luminophores in solution although Núñez and co-workers have demonstrated that non-conjugated carborane luminophores are appreciably luminescent.^{8,14,16} The non-emissive nature was attributed to the variable nature of C–C bond of *o*-carborane,¹⁷ which dissipates the excited state energy *via* a nonradiative decay process in solution. In contrast, the solid or film state becomes emissive due to the restricted rotation of the carborane moiety, resulting in the AIE phenomenon.¹⁸ As has been shown by Chujo and co-workers (1), such AIE can be useful for the emission color tuning.⁹

In a continuous effort to investigate the photophysical properties of carborane-containing luminophores and the emission color tuning, we newly designed di-*o*-carborane substituted benzene compounds (1–4), in which aryl-*o*-carborane cages are introduced at the 1 and 4 positions of the phenylene ring. By the electronic variation of the substituent on the appended aryl group at the C1-position of *o*-carborane from electron-withdrawing to electron-donating properties, we intended to achieve color tuning of AIE. We observed the occurrence of “through-space” CT between the appended aryl group and the central phenylene ring and found that the emission color of the CT transition can also be tuned by changing the aryl substituent. The detailed synthesis, characterization, and luminescent properties of 1–4 are described with theoretical calculations.

Results and discussion

Synthesis and characterization

The starting bis-acetylene compounds 1a–4a were readily obtained from Sonogashira coupling reaction between 1,4-diiodobenzene and various arylacetylene derivatives (Scheme 1).



Scheme 1 Synthesis of 1,4-di-(1-Ar-*o*-carboran-2-yl)benzene (1–4). Conditions and reagents: (i) CuI, PdCl₂(PPh₃)₂, NEt₃–toluene, r.t., 24 h, 58–88% (1a–4a). (ii) B₁₀H₁₄, Et₂S, toluene, 110 °C, 3 d, 6.0–68% (1–4).

The substituted aryl group with an electron-withdrawing (CF₃) or -donating (*n*-Bu, NMe₂) moiety was introduced to modulate the electronic effect with respect to the phenyl substituted compound. The final di-carborane compounds 1–4 were prepared from the cage forming reaction of decaborane (B₁₀H₁₄) with the bis-acetylene precursors (1a–4a) in the presence of Et₂S^{19,20} following the modified literature procedures for 2.¹⁹ Compounds 1, 3, and 4 have been characterized by NMR spectroscopy, elemental analysis, and the X-ray diffraction method. The ¹¹B NMR signals detected in the regions of δ –1 to –12 ppm confirm the presence of *o*-carboranyl boron atoms. Single crystals of 1, 3, and 4 suitable for X-ray diffraction studies were obtained from slow evaporation of an acetone (or THF)/MeOH solution at room temperature.† As shown in Fig. 1, the carborane cages are held at the *para*-positions of the central phenylene ring. The two aryl groups on the C1-carborane carbon atoms are oppositely positioned, featuring C₂-symmetry probably due to the steric reason. The aryl and phenylene rings on the C1 and C2 atoms, respectively, are oriented roughly perpendicular to the plane defined by C_{Ar}–C₁–C₂–C_{Ph} (avg angles: 58.2°/74.0° for 1, 87.6°/85.4° for 3, 76.7°/73.4° for 4), as has been similarly observed in other diarylcarborane compounds,²¹ indicating the existence of π -interaction between the aryl π -system and the anti-bonding C–C orbital ($\sigma^*(C-C)$) of cage carbon atoms.¹⁷ Indeed, the C1–C2 bond length increases with the increasing order of the electron-donating effect of an aryl group (1.711(6) and 1.718(5) Å for 1, 1.729(3) Å for 3, 1.779(3) and 1.758(3) Å for 4), supporting the appreciable π -interaction.^{9,17}

Optical properties

To examine the optical properties, UV-vis absorption and photoluminescence (PL) experiments were carried out with 1–4 in both solution and solid state. All the compounds feature major absorption bands in the region of 200–250 nm with the vibronic structure assignable to π – π^* transition in the central phenylene ring and the appended aryl group (Fig. 2 and Table 2). In particular, the absorption bands of 1–3 accompany small low-energy absorption bands at around 275 nm which tails to 300 nm. These bands could be tentatively assigned to intramolecular $\pi(\text{aryl}) \rightarrow \pi^*(\text{phenylene})$ charge transfer (CT) transition. In 4, the intense low-energy absorption band centered at $\lambda_{\text{abs}} = 286$ nm, which accompanies a broad tail at 350–400 nm, is clearly observed. The structureless band shape also suggests that the absorption is mainly originated from $\pi(\text{aryl}) \rightarrow \pi^*(\text{phenylene})$ CT transition, in which the lone pair electrons of nitrogen atom would have a large contribution to the aryl donation (see TD-DFT results).

Next, the emission properties of 1–4 were investigated by PL measurements (Fig. 3 and Table 2). Compounds 1–4 show virtually no emission in solution, as usually observed in other *o*-carborane substituted luminophores.^{3,4,7–9,11,12,22} This phenomenon could be related to the involvement of *o*-carborane in the excited states, which facilitates the nonradiative decay process due to the variable nature of C–C bond of carborane in solution.¹⁷ From the absorption spectra, it was

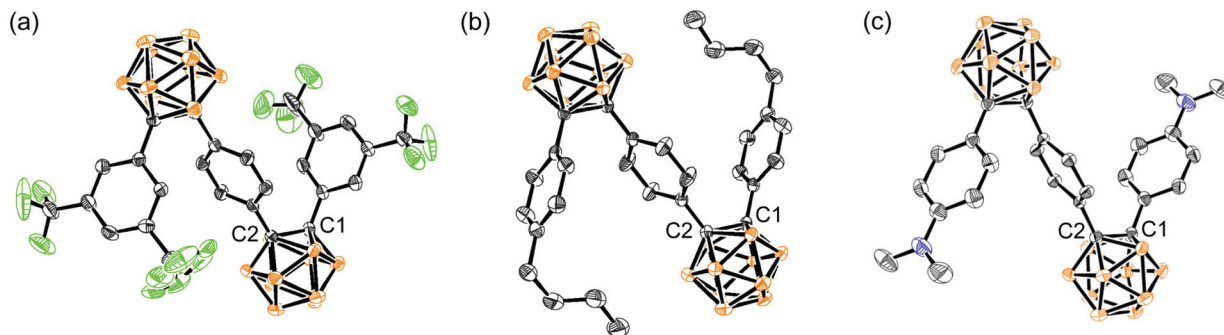


Fig. 1 Crystal structures of (a) 1, (b) 3, and (c) 4. H-atoms are omitted for clarity. Due to the disorder of three fluorine atoms of one CF_3 group in 1, the fluorine atoms were partitioned. Color code: blue = nitrogen; green = fluorine; orange = boron atom.

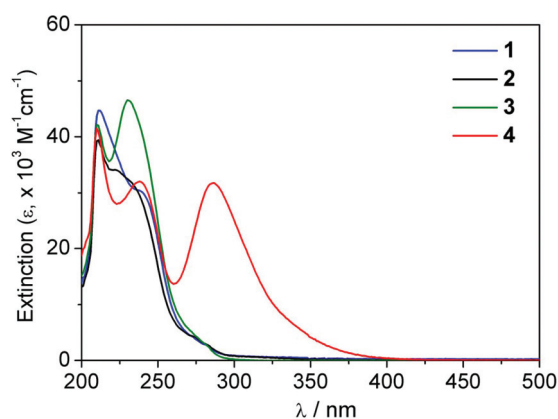


Fig. 2 UV-vis absorption spectra of 1–4 in THF ($\text{ca. } 2 \times 10^{-5} \text{ M}$).

suggested that the lowest-energy excited state in 1–4 is mainly charge transfer in nature from the appended aryl group to the central phenylene ring. Because the two carborane cages are conjugated with the phenylene ring, the CT state may have a substantial contribution from the carboranes, leading to the emission quenching in solution. In contrast, 1–4 exhibit an intense emission over the region ranging from 400 to 700 nm in a rigid matrix at 77 K and in the solid state, such as a film and a powder, *i.e.*, aggregation-induced emission (AIE) is observed (Fig. 3a–c). This result can be attributed to the restricted rotation of the carborane moiety in the solid state, which prevents the variation in the C–C bond of carborane.⁵ The AIE phenomenon can also be observed from a THF–water (1 : 99, v/v) mixture (Fig. 3d). Most interestingly, the emission wavelengths of 1–4 exhibit an apparent shift depending on the substituent of the aryl group under all measurement conditions although the difference in the wavelength between 2 (H) and 3 (*n*-Bu) is relatively marginal. While compound 1 bearing the electron-withdrawing CF_3 shows the emission at a high energy region (478–510 nm), the PL spectra are gradually red-shifted upon changing the substituent from CF_3 to the electron-donating NMe_2 group (from 1 to 4). Since the HOMO localized in the aryl moiety should be more affected by the substituent in comparison with the LUMO which is mostly located on the phenylene ring, the emission color could be

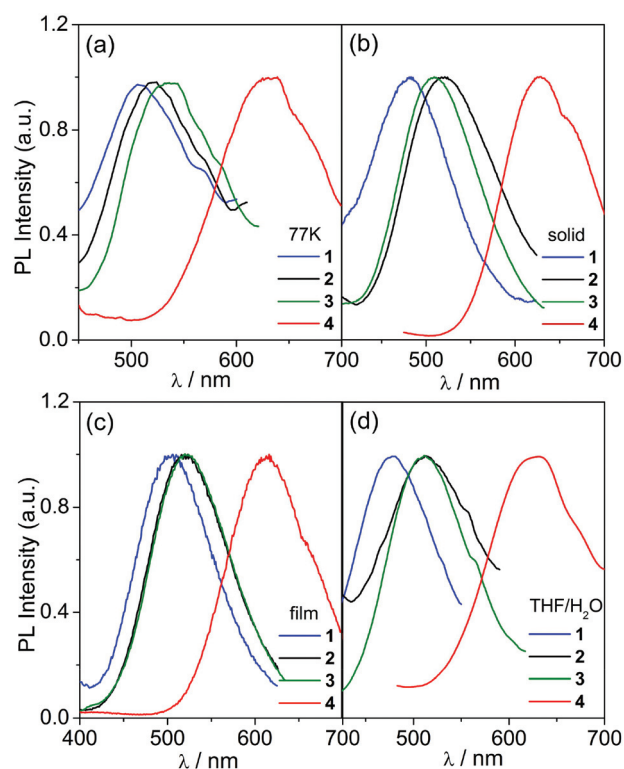


Fig. 3 PL spectra of 1–4 (a) at 77 K ($5 \times 10^{-5} \text{ M}$ in THF), (b) in the film state (10 wt% in PMMA), (c) in the neat solid state, and (d) in a THF– H_2O mixture (1 : 99, v/v, $5 \times 10^{-5} \text{ M}$).

tuned by the change of the HOMO–LUMO energy gap (see DFT results). This finding further suggests that the emission originates from the intramolecular “through-space” CT transition²³ between the appended aryl group and the central phenylene ring. Although the observed emission color tuning is similar to that observed in the mono-carborane compounds, such as bis(4-phenylethynyl)phenyl-*o*-carborane (I), the aryl groups in those compounds are directly conjugated with a carborane cage. Thus the excited state was characterized to be π – π^* transition with a substantial intramolecular CT character.⁹ In contrast, the present di-*o*-carborane system utilizes discrete $\pi \rightarrow \pi^*$ charge transfer from the appended aryl donor to the

phenylene acceptor which is conjugated with carborane. The observed emission features for **1–4** further indicate that the electronic alteration of the aryl group at the C1-position of *o*-carborane can lead to facile tuning of the emission color.

Theoretical calculation

To elucidate the nature of electronic transition and emission color tuning properties, TD-DFT calculations on the ground state geometry (S_0) of **1–4** were performed at the B3LYP/6-31G(d) level of theory (Fig. 4 and Table 3). It can be seen that the lowest energy absorption in **1–4** is mainly characterized by HOMO–LUMO transition. The LUMO in **1–4** is delocalized over the central phenylene ring and carboranyl carbon atoms. The contribution from the carborane cage to LUMO is found to be substantial (23–28%). Interestingly, while the HOMO in **2–4** bears a major contribution from the appended aryl group, the HOMO and HOMO–1 in **1** are localized in the central phenylene ring. This result could be attributed to the strong electron-withdrawing effect of the two CF_3 groups of the appended aryl group in **1**, leading to the greater stabilization of the π level of the aryl group than that of the central phenylene group. Consequently, the HOMO–LUMO transition in **2–4** is mainly assignable to the $\pi(\text{aryl}) \rightarrow \pi^*(\text{phenylene})$ CT transition while **1** has a major contribution from the $\pi\text{--}\pi^*$ transition centered on the phenylene group. Nevertheless, owing to the large contribution of the carborane to LUMO in **1**, the $\pi\text{--}\pi^*$ transition may also have a substantial charge-transfer character, similar to that observed for bis(4-phenylethynyl)phenyl-*o*-carborane compounds (**1**).⁹ Since the computed oscillator strength (f_{calc}) of the lowest energy transition in **1–4** is found to be weak ($f_{\text{calc}} \approx 0.1$), it is likely that the transition appears as a weak shoulder or a tail in the absorption spectra (Fig. 2). The

computed position of the absorption band correlates well with the electronic property of the substituent on the appended aryl group in such a way that the band position is bathochromically shifted with the electron-donating substituent (**1** \rightarrow **4**) although the experimental shift in the absorption spectra was not apparently distinguished among **1–3** in the region of *ca.* 275 nm, presumably due to overlapping with other higher energy bands. In contrast, the computed absorption wavelength of 395 nm for **4** falls in the lower energy absorption region (<400 nm). Moreover, the TD-DFT calculation indicates that the shift in the absorption wavelength is mainly attributed to the change in the HOMO level depending on the substituent. As shown in Fig. 4, while the LUMO levels of **1–4** are very slightly changed, the HOMO levels gradually increase with the increasing electron-donating effect of the substituent. This finding is also consistent with the change in the emission wavelength. As shown in Fig. 3, the emission wavelengths of **1–4** exhibited a gradual red shift with the electron-donating substituent on going from **1** to **4**. Because of the reduction of a band gap due to the greater elevation of the HOMO level than that of the LUMO, the compounds with the more electron-donating substituent result in the more red-shifted emission. These results thus suggest that the introduction of a substituent to the appended aryl ring of *o*-carborane can also allow the color tuning of AIE by the change of the HOMO–LUMO energy gap.

Experimental

General considerations

All operations were performed under an inert nitrogen atmosphere using the standard Schlenk and glove box techniques.

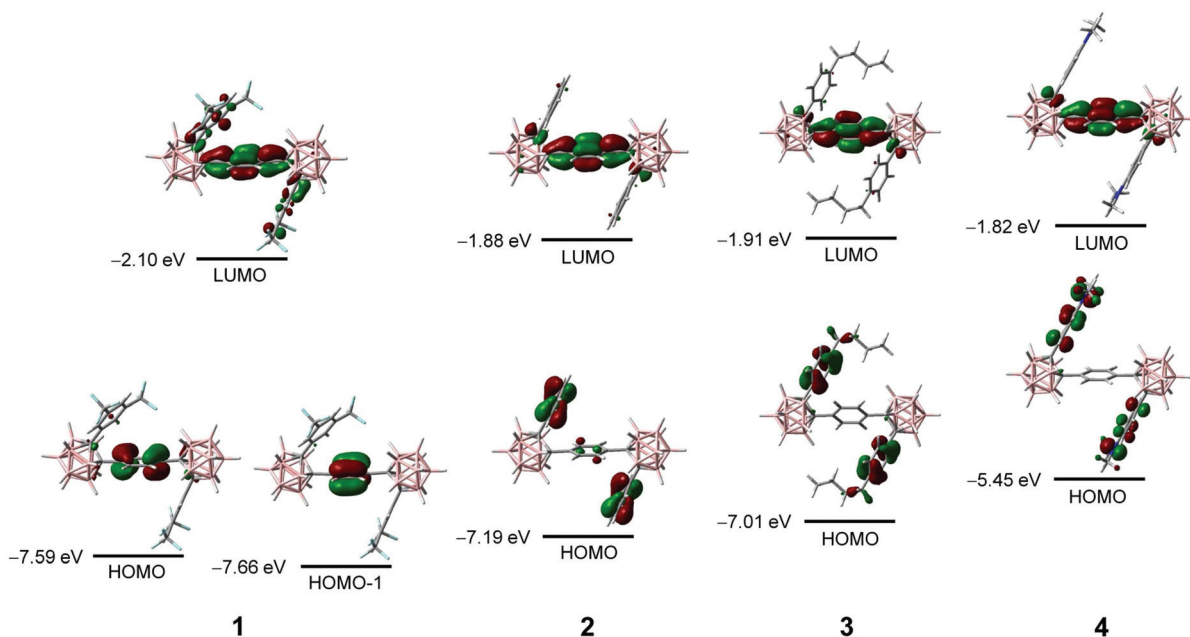


Fig. 4 HOMO and LUMO of **1–4** at the S_0 geometries (isovalue = 0.04).

Anhydrous grade solvents (Aldrich) were dried by passing them through an activated alumina column and stored over activated molecular sieves (5 Å). Spectrophotometric-grade tetrahydrofuran (THF) was used as received from Aldrich. Commercial reagents were used without any further purification after purchasing from Aldrich (bis(triphenylphosphine)-palladium(II) dichloride, copper(I) iodide, diethyl sulfide, triethylamine, 1,4-diiodobenzene, 1-ethynyl-3,5-bis(trifluoromethyl)benzene, 4-ethynyl-*N,N*-dimethylaniline, phenylacetylene, 1-butyl-4-ethynylbenzene) and KatChem ($B_{10}H_{14}$, decaborane). **2a**, **2**,¹⁹ and **4a**²⁴ were synthesized according to the modified literature procedures. Deuterated solvents from Cambridge Isotope Laboratories were used. NMR spectra of compounds were recorded on a Bruker Avance 400 spectrometer (400.13 MHz for 1H , 100.62 MHz for ^{13}C , 128.38 MHz for ^{11}B) at ambient temperature. Chemical shifts are given in ppm, and are referenced against external Me_4Si (1H , ^{13}C) and $BF_3 \cdot Et_2O$ (^{11}B). Elemental analyses were performed on an EA1110 (Fisons Instruments) by the Environmental Analysis Laboratory at KAIST. UV-vis absorption and PL spectra were recorded on a Jasco V-530 and a Spex Fluorog-3 Luminescence spectrophotometer, respectively.

Synthesis of 1a. Toluene (10 mL) and triethylamine (90 mL) were added *via* cannula to the mixture of 1,4-diiodobenzene (1.16 g, 3.52 mmol), copper(I) iodide (65 mg), and $Pd(PPh_3)_2Cl_2$ (125 mg) at room temperature. After stirring for 15 min, 1-ethynyl-3,5-bis(trifluoromethyl)benzene (1.6 mL, 7.78 mmol) was added to the resulting dark brown slurry. The reaction mixture was then stirred for 24 h. The volatiles were removed using a rotary evaporator affording dark gray residue. After washing with MeOH followed by *n*-hexane, the remaining solid was dried at room temperature, which afforded a sky blue solid (1.40 g, 72.3%). 1H NMR (THF- d_8): δ 8.17 (s, 4 H, aryl), 8.06 (s, 2 H, aryl), 7.66 (s, 4 H, phenylene). ^{13}C NMR (THF- d_8): δ 132.84, 132.83, 132.65, 126.36, 124.16, 123.82, 122.95, 92.69 (acetylene), 89.25 (acetylene). Anal. Calcd for $C_{26}H_{10}F_{12}$: C, 56.74; H, 1.83. Found: C, 56.66; H, 1.74.

Synthesis of 3a. A procedure analogous to that for **1a** was employed with 1,4-diiodobenzene (2.00 g, 6.06 mmol), copper(I) iodide (115 mg), $Pd(PPh_3)_2Cl_2$ (200 mg), and 1-butyl-4-ethynylbenzene (2.35 mL, 13.34 mmol) to afford **3a** as a gray powder (2.08 g, 88.0%). 1H NMR ($CDCl_3$): δ 7.47 (s, 4 H, phenylene), 7.43 (d, $J = 7.9$ Hz, 4 H, aryl), 7.15 (d, $J = 7.9$ Hz, 4 H, aryl), 2.61 (t, $J = 7.4$ Hz, 4 H, *n*-Bu), 1.63–1.55 (m, 4 H, *n*-Bu), 1.39–1.30 (m, 4 H, *n*-Bu), 0.92 (t, $J = 7.1$ Hz, 6 H, *n*-Bu). ^{13}C NMR ($CDCl_3$): δ 143.61, 131.51, 131.43, 128.50, 123.12, 120.16, 91.39 (acetylene), 88.53 (acetylene), 35.61 (*n*-Bu), 33.37 (*n*-Bu), 22.30 (*n*-Bu), 13.92 (*n*-Bu). Anal. Calcd for $C_{30}H_{30}$: C, 92.26; H, 7.74. Found: C, 91.94; H, 8.31.

Synthesis of 1. This compound was prepared using an analogous method described previously.^{19,20} To a toluene solution (50 mL) of decaborane ($B_{10}H_{14}$, 3.27 mmol) and **1a** (0.75 g, 1.69 mmol) was added an excess amount of Et_2S (5 equiv.) at room temperature. After heating to reflux, the reaction mixture was further stirred for 3 days. The solvent was removed under vacuum and MeOH (50 mL) was added. The resulting yellow

solid was filtered and re-dissolved in toluene. The solution was purified by passing through an alumina column and the solvent was removed *in vacuo* affording **1** as a white solid. Recrystallization from a mixed solvent of acetone–MeOH gave 0.72 g of **1** (67.6%). Single crystals suitable for the X-ray diffraction study were obtained by slow evaporation of an acetone–MeOH solution of **1**. 1H NMR ($CDCl_3$): δ 7.73 (s, 2 H, aryl), 7.69 (s, 4 H, aryl), 7.27 (s, 4 H, phenylene), 3.80–1.60 (br, 20 H, B–H). ^{13}C NMR ($CDCl_3$): δ 132.86, 132.73, 131.13, 130.81, 130.19, 124.06, 122.28, 82.99 (CB–C), 81.42 (CB–C). ^{11}B NMR ($CDCl_3$): δ –1.3 (br s, 4B), –9.3 (br s, 16B). Anal. Calcd for $C_{26}H_{30}B_{20}F_{12}$: C, 39.69; H, 3.84. Found: C, 39.90; H, 3.74.

Synthesis of 3. A procedure analogous to that for **1** was employed with decaborane ($B_{10}H_{14}$, 9.92 mmol), **3a** (1.50 g, 3.84 mmol), and Et_2S (5 equiv.). Recrystallization from a mixed solvent of acetone–MeOH afforded **3** as a white solid (1.06 g, 44.2%). Single crystals suitable for X-ray diffraction study were obtained by slow evaporation of an acetone–MeOH solution of **3**. 1H NMR ($CDCl_3$): δ 7.15 (d, $J = 8.3$ Hz, 4 H, phenylene), 7.09 (s, 4 H, aryl), 6.87 (d, $J = 8.4$ Hz, 4 H, aryl), 3.20–1.60 (br, 20 H, B–H) 2.49 (t, $J = 7.5$ Hz, 4 H, *n*-Bu), 1.52–1.44 (m, 4 H, *n*-Bu), 1.28–1.18 (m, 4 H, *n*-Bu), 0.88 (t, $J = 7.2$ Hz, 6 H, *n*-Bu). ^{13}C NMR ($CDCl_3$): δ 145.53, 132.57, 130.35, 130.09, 128.32, 127.56, 85.28 (CB–C), 83.02 (CB–C), 35.01 (*n*-Bu), 33.14 (*n*-Bu), 22.13 (*n*-Bu), 13.87 (*n*-Bu). ^{11}B NMR ($CDCl_3$): δ –2.6 (br s, 4B), –10.2 (br s, 16B). Anal. Calcd for $C_{30}H_{50}B_{20}$: C, 57.47; H, 8.04. Found: C, 57.72; H, 8.28.

Synthesis of 4. A procedure analogous to that for **1** was employed with decaborane ($B_{10}H_{14}$, 6.58 mmol), **4a** (1.00 g, 2.74 mmol), and Et_2S (5 equiv.). Recrystallization from a mixed solvent of acetone–MeOH afforded **4** as a yellow solid (0.11 g, 6.7%). Single crystals suitable for X-ray diffraction study were obtained by slow evaporation of a THF–MeOH solution of **4**. 1H NMR (THF- d_8): δ 7.48 (s, 4 H, phenylene), 7.35 (d, $J = 8.7$ Hz, 4 H, aryl), 6.61 (d, $J = 8.7$ Hz, 4 H, aryl), 3.08 (s, 12 H, NMe_2), 3.80–1.60 (br, 20 H, B–H). ^{13}C NMR (THF- d_8): δ 152.45, 133.84, 132.33, 131.32, 117.93, 111.75, 89.05 (CB–C), 85.21 (CB–C), 39.92 (NMe_2). ^{11}B NMR (THF- d_8): δ –4.3, –5.6 (br s, 4B), –11.3, –12.4 (br s, 16B). Anal. Calcd for $C_{26}H_{44}B_{20}N_2$: C, 51.97; H, 7.38; N, 4.66. Found: C, 51.43; H, 7.58; N, 4.37.

X-ray crystallography

A specimen of suitable size and quality was coated with Paratone oil and mounted onto a glass capillary. The crystallographic measurement was performed using a Bruker Apex II-CCD area detector diffractometer, with graphite-monochromated $MoK\alpha$ radiation ($\lambda = 0.71073$ Å). The structure was solved by direct methods and all nonhydrogen atoms were subjected to anisotropic refinement by full-matrix least-squares on F^2 by using the SHELXTL/PC package.²⁵ Hydrogen atoms were placed at their geometrically calculated positions and were refined riding on the corresponding carbon atoms with isotropic thermal parameters. In the case of compound **1**, three fluorine atoms (F7–F9) of one CF_3 group were disordered, so the fluorine atoms were partitioned. The detailed crystallographic data are given in Table 1.

Table 1 Crystallographic data and parameters for **1**, **3**, and **4**

Compound	1	3	4
Formula	C ₂₆ H ₃₀ B ₂₀ F ₁₂	C ₃₀ H ₅₀ B ₂₀	C ₂₆ H ₄₄ B ₂₀ N ₂
Formula weight	786.70	626.90	600.83
Crystal system	Monoclinic	Monoclinic	Monoclinic
Space group	<i>P</i> 2 ₁	<i>P</i> 2 ₁ / <i>n</i>	<i>P</i> 2 ₁ / <i>c</i>
<i>a</i> (Å)	8.7298(5)	11.932(2)	17.770(4)
<i>b</i> (Å)	22.0835(12)	13.890(2)	13.153(3)
<i>c</i> (Å)	10.9754(6)	13.636(2)	15.181(4)
α (°)	90	90	90
β (°)	112.501(2)	114.132(11)	102.535(10)
γ (°)	90	90	90
<i>V</i> (Å ³)	1954.81(19)	2062.4(6)	3463.7(15)
<i>Z</i>	2	2	4
ρ_{calc} (g cm ⁻³)	1.337	1.009	1.152
μ (mm ⁻¹)	0.109	0.049	0.057
<i>F</i> (000)	788	660	1256
<i>T</i> (K)	296	296	296
Scan mode	<i>Multi</i>	<i>Multi</i>	<i>Multi</i>
<i>hkl</i> range	−10 → +10, −25 → +24, −12 → +12	−14 → +14, −16 → +16, −16 → +16	−19 → +19, −14 → +14, −16 → +16
Measd reflns	27 490	16 740	38 848
Unique reflns [<i>R</i> _{int}]	6038 [0.0547]	3926 [0.0394]	4825 [0.1126]
Reflns used for refinement	6038	3926	4825
Refined parameters	551	267	437
<i>R</i> ₁ ^a (<i>I</i> > 2σ(<i>I</i>))	0.0593	0.0820	0.0488
w <i>R</i> ₂ ^b all data	0.1861	0.2733	0.1441
GOF on <i>F</i> ²	1.017	1.077	1.012
ρ_{fin} (max/min) (e Å ⁻³)	0.299, −0.268	0.557, −0.335	0.156, −0.188

$${}^a R_1 = \sum ||F_o| - |F_c|| / \sum |F_o|. {}^b wR_2 = \{[\sum w(F_o^2 - F_c^2)^2] / [\sum w(F_o^2)^2]\}^{1/2}.$$

Table 2 UV-vis absorption and PL data for **1–4**

Compound	$\lambda_{\text{abs}}/\text{nm}^a$ ($\epsilon \times 10^{-3}/\text{M}^{-1} \text{cm}^{-1}$)	$\lambda_{\text{em}}/\text{nm}$				
		298 K ^b	77 K ^b	Solid	Film ^c	THF-H ₂ O ^d
1	212 (44.7), 238 (30.4)	—	510	483	506	478
2	211 (39.4), 223 (34.0)	—	520	521	520	513
3	210 (42.1), 231 (46.5)	—	539	509	521	511
4	210 (41.5), 238 (32.0), 286 (31.7)	—	639	625	616	631

^a Measured in degassed THF (*ca.* 2 × 10⁻⁵ M). ^b Measured in degassed THF (5 × 10⁻⁵ M). ^c Spin-coated PMMA film with **1–4** (10 wt%). ^d In THF-H₂O = 1 : 99 (v/v). λ_{exc} = 324 nm for **1**; 325 nm for **2**; 333 nm for **3**; 360 nm for **4**.

UV-vis absorption and PL measurements

The solution UV-vis absorption and PL measurements were performed in degassed THF with a 1 cm quartz cuvette. PL measurements were also carried out under various conditions, such as at 77 K, in the film state, and in the neat solid state. The detailed conditions are given in Table 2.

Table 3 The lowest singlet excited states for **1–4** from TD-DFT calculations^a

	States	λ_{calc}	f_{calc}	Assignment
1	S ₁	256.6	0.0661	HOMO−1 → LUMO (60.0%) HOMO → LUMO (19.9%)
2	S ₁	262.7	0.0979	HOMO → LUMO (90.0%)
3	S ₁	273.9	0.0903	HOMO → LUMO (98.0%)
4	S ₁	395.2	0.1218	HOMO → LUMO (98.8%)

^a Singlet energies for the vertical transition calculated at the optimized S₀ geometries.

Theoretical calculations

The geometries of the ground (S₀) state of **1–4** were optimized using the density functional theory (DFT) method. The electronic transition energies including electron correlation effects were computed by the time dependent density functional theory (TD-DFT)²⁶ method using the B3LYP²⁷ functional (B3LYP). The 6-31G(d) basis set²⁸ was used for all atoms. To include the solvation effect of THF, the polarizable continuum model (PCM) was used in the calculations. All calculations were carried out using the GAUSSIAN 09 program.²⁹

Conclusions

1,4-Di-*o*-carborane substituted benzene compounds (**1–4**), in which aryl-*o*-carborane cages are introduced at the 1 and 4 positions of phenylene ring, were prepared and characterized. The electronic variation of the substituent on the appended aryl group at the C1-position of *o*-carborane led to the color tuning of the aggregation-induced emission. Experimental and theoretical calculation results suggested that intramolecular “through-space” charge transfer occurs between the appended aryl group (HOMO) and the central phenylene ring (LUMO), and the greater change in the HOMO level by the substituent than that in the LUMO is responsible for the emission color tuning. The results in this study indicate that the emission color of the *o*-carborane-containing luminophores can also be tuned by changing the appended aryl group of *o*-carborane.

Acknowledgements

This work was supported by the Basic Science Research Program (no. 2012039773 for M. H. Lee) and the Priority Research Centers program (no. 2009-0093818 for M. H. Lee) through the National Research Foundation of Korea (NRF). Computational resources for this work were provided by the KISTI (KSC-2012-C2-42).

Notes and references

- 1 H. J. Bae, H. Kim, K. M. Lee, T. Kim, M. Eo, Y. S. Lee, Y. Do and M. H. Lee, *Dalton Trans.*, 2013, **42**, 8549–8552.

- 2 C. Shi, H. Sun, Q. Jiang, Q. Zhao, J. Wang, W. Huang and H. Yan, *Chem. Commun.*, 2013, **49**, 4746–4748; M. Eo, H. J. Bae, M. Hong, Y. Do, S. Cho and M. H. Lee, *Dalton Trans.*, 2013, **42**, 8104–8112; L. Weber, J. Kahlert, L. Böhling, A. Brockhinke, H.-G. Stammer, B. Neumann, R. A. Harder, P. J. Low and M. A. Fox, *Dalton Trans.*, 2013, **42**, 2266–2281; N. S. Hosmane, *Boron Science: New Technologies and Applications*, CRC Press, New York, 2012; J. J. Peterson, Y. C. Simon, E. B. Coughlin and K. R. Carter, *Chem. Commun.*, 2009, 4950–4952.
- 3 T. Kim, H. Kim, K. M. Lee, Y. S. Lee and M. H. Lee, *Inorg. Chem.*, 2013, **52**, 160–168.
- 4 K. C. Song, H. Kim, K. M. Lee, Y. S. Lee, Y. Do and M. H. Lee, *Dalton Trans.*, 2013, **42**, 2351–2354; K. M. Lee, J. O. Huh, T. Kim, Y. Do and M. H. Lee, *Dalton Trans.*, 2011, **40**, 11758–11764.
- 5 L. Weber, J. Kahlert, R. Brockhinke, L. Böhling, A. Brockhinke, H.-G. Stammer, B. Neumann, R. A. Harder and M. A. Fox, *Chem.–Eur. J.*, 2012, **18**, 8347–8357.
- 6 Y. Morisaki, M. Tominaga and Y. Chujo, *Chem.–Eur. J.*, 2012, **18**, 11251–11257; K.-R. Wee, Y.-J. Cho, S. Jeong, S. Kwon, J.-D. Lee, I.-H. Suh and S. O. Kang, *J. Am. Chem. Soc.*, 2012, **134**, 17982–17990; K. Kokado and Y. Chujo, *Dalton Trans.*, 2011, **40**, 1919–1923; A. M. Prokhorov, P. A. Slepukhin, V. L. Rusinov, V. N. Kalinin and D. N. Kozhevnikov, *Chem. Commun.*, 2011, **47**, 7713–7715; M. H. Park, K. M. Lee, T. Kim, Y. Do and M. H. Lee, *Chem.–Asian J.*, 2011, **6**, 1362–1366; K. Kokado, M. Tominaga and Y. Chujo, *Macromol. Rapid Commun.*, 2010, **31**, 1389–1394; K. Kokado and Y. Chujo, *Macromolecules*, 2009, **42**, 1418–1420; K. Kokado, Y. Tokoro and Y. Chujo, *Macromolecules*, 2009, **42**, 2925–2930; K. Kokado, Y. Tokoro and Y. Chujo, *Macromolecules*, 2009, **42**, 9238–9242.
- 7 K.-R. Wee, W.-S. Han, D. W. Cho, S. Kwon, C. Pac and S. O. Kang, *Angew. Chem., Int. Ed.*, 2012, **51**, 2677–2680.
- 8 A. Ferrer-Ugalde, E. J. Juárez-Pérez, F. Teixidor, C. Viñas, R. Sillanpää, E. Pérez-Inestrosa and R. Núñez, *Chem.–Eur. J.*, 2012, **18**, 544–553.
- 9 K. Kokado and Y. Chujo, *J. Org. Chem.*, 2011, **76**, 316–319.
- 10 B. P. Dash, R. Satapathy, J. A. Maguire and N. S. Hosmane, *New J. Chem.*, 2011, **35**, 1955–1972.
- 11 B. P. Dash, R. Satapathy, E. R. Gaillard, K. M. Norton, J. A. Maguire, N. Chug and N. S. Hosmane, *Inorg. Chem.*, 2011, **50**, 5485–5493; B. P. Dash, R. Satapathy, E. R. Gaillard, J. A. Maguire and N. S. Hosmane, *J. Am. Chem. Soc.*, 2010, **132**, 6578–6587.
- 12 F. Lerouge, A. Ferrer-Ugalde, C. Viñas, F. Teixidor, R. Sillanpää, A. Abreu, E. Xochitiotzi, N. Farfán, R. Santillan and R. Núñez, *Dalton Trans.*, 2011, **40**, 7541–7550.
- 13 J. O. Huh, H. Kim, K. M. Lee, Y. S. Lee, Y. Do and M. H. Lee, *Chem. Commun.*, 2010, **46**, 1138–1140.
- 14 F. Lerouge, C. Viñas, F. Teixidor, R. Núñez, A. Abreu, E. Xochitiotzi, R. Santillan and N. Farfán, *Dalton Trans.*, 2007, 1898–1903.
- 15 R. N. Grimes, *Carboranes*, Academic Press, London, 2011; Z. Chen and R. B. King, *Chem. Rev.*, 2005, **105**, 3613–3642; R. B. King, *Chem. Rev.*, 2001, **101**, 1119–1152; M. F. Hawthorne, in *Advances in Boron Chemistry: Special Publication No. 201*, Royal Society of Chemistry, London, 1997, p. 261; R. E. Williams, *Chem. Rev.*, 1992, **92**, 177–207; V. I. Bregadze, *Chem. Rev.*, 1992, **92**, 209–223.
- 16 A. González-Campo, A. Ferrer-Ugalde, C. Viñas, F. Teixidor, R. Sillanpää, J. Rodríguez-Romero, R. Santillan, N. Farfán and R. Núñez, *Chem.–Eur. J.*, 2013, **19**, 6299–6312.
- 17 J. M. Oliva, N. L. Allan, P. v. R. Schleyer, C. Viñas and F. Teixidor, *J. Am. Chem. Soc.*, 2005, **127**, 13538–13547; I. V. Glukhov, M. Y. Antipin and K. A. Lyssenko, *Eur. J. Inorg. Chem.*, 2004, **2004**, 1379–1384; J. Llop, C. Viñas, J. M. Oliva, F. Teixidor, M. A. Flores, R. Kivekas and R. Sillanpää, *J. Organomet. Chem.*, 2002, **657**, 232–238; J. Llop, C. Viñas, F. Teixidor, L. Victori, R. Kivekäs and R. Sillanpää, *Organometallics*, 2001, **20**, 4024–4030.
- 18 Y. Hong, J. W. Y. Lam and B. Z. Tang, *Chem. Soc. Rev.*, 2011, **40**, 5361–5388; Y. Hong, J. W. Y. Lam and B. Z. Tang, *Chem. Commun.*, 2009, 4332–4353; J. Liu, J. W. Y. Lam and B. Z. Tang, *Chem. Rev.*, 2009, **109**, 5799–5867; J. Chen, C. C. W. Law, J. W. Y. Lam, Y. Dong, S. M. F. Lo, I. D. Williams, D. Zhu and B. Z. Tang, *Chem. Mater.*, 2003, **15**, 1535–1546.
- 19 C. Songkram, K. Takaishi, K. Yamaguchi, H. Kagechika and Y. Endo, *Tetrahedron Lett.*, 2001, **42**, 6365–6368.
- 20 W. Jiang, C. B. Knobler and M. F. Hawthorne, *Inorg. Chem.*, 1996, **35**, 3056–3058; T. E. Paxson, K. P. Callahan and M. F. Hawthorne, *Inorg. Chem.*, 1973, **12**, 708–709; M. F. Hawthorne, T. E. Berry and P. A. Wegner, *J. Am. Chem. Soc.*, 1965, **87**, 4746–4750; T. L. Heying, J. W. Ager, S. L. Clark, D. J. Mangold, H. L. Goldstein, M. Hillman, R. J. Polak and J. W. Szymanski, *Inorg. Chem.*, 1963, **2**, 1089–1092.
- 21 M. A. Fox, C. Nervi, A. Crivello, A. S. Batsanov, J. A. K. Howard, K. Wade and P. J. Low, *J. Solid State Electrochem.*, 2009, **13**, 1483–1495; L. A. Boyd, W. Clegg, R. C. B. Copley, M. G. Davidson, M. A. Fox, T. G. Hibbert, J. A. K. Howard, A. Mackinnon, R. J. Peace and K. Wade, *Dalton Trans.*, 2004, 2786–2799; E. S. Alekseyeva, M. A. Fox, J. A. K. Howard, J. A. H. MacBride and K. Wade, *Appl. Organomet. Chem.*, 2003, **17**, 499–508; P. T. Brain, J. Cowie, D. J. Donohoe, D. Hnyk, D. W. H. Rankin, D. Reed, B. D. Reid, H. E. Robertson, A. J. Welch, M. Hofmann and P. v. R. Schleyer, *Inorg. Chem.*, 1996, **35**, 1701–1708; Z. G. Lewis and A. J. Welch, *Acta Crystallogr.*, 1993, **49**, 705–710.
- 22 Y. C. Simon, J. J. Peterson, C. Mangold, K. R. Carter and E. B. Coughlin, *Macromolecules*, 2008, **42**, 512–516.
- 23 I. Ciofini, T. Le Bahers, C. Adamo, F. Odobel and D. Jacquemin, *J. Phys. Chem. C*, 2012, **116**, 11946–11955; L. Zhu, C. Zhong, Z. Liu, C. Yang and J. Qin, *Chem. Commun.*, 2010, **46**, 6666–6668; D. I. Schuster, K. Li, D. M. Guldi, A. Palkar, L. Echegoyen, C. Stanisky, R. J. Cross, M. Niemi, N. V. Tkachenko and

- H. Lemmetyinen, *J. Am. Chem. Soc.*, 2007, **129**, 15973–15982; H. Wu, D. Zhang, L. Su, K. Ohkubo, C. Zhang, S. Yin, L. Mao, Z. Shuai, S. Fukuzumi and D. Zhu, *J. Am. Chem. Soc.*, 2007, **129**, 6839–6846.
- 24 P. Nguyen, Z. Yuan, L. Agocs, G. Lesley and T. B. Marder, *Inorg. Chim. Acta*, 1994, **220**, 289–296.
- 25 G. M. Sheldrick, *SHELXL-93: Program for the refinement of crystal structures*, University of Göttingen, Germany, 1993.
- 26 E. Runge and E. K. U. Gross, *Phys. Rev. Lett.*, 1984, **52**, 997–1000.
- 27 P. J. Stephens, F. J. Devlin, C. F. Chabalowski and M. J. Frisch, *J. Phys. Chem.*, 1994, **98**, 11623–11627; C. Lee, W. Yang and R. G. Parr, *Phys. Rev. B: Condens. Matter*, 1988, **37**, 785–789.
- 28 M. M. Francl, W. J. Pietro, W. J. Hehre, J. S. Binkley, M. S. Gordon, D. J. DeFrees and J. A. Pople, *J. Chem. Phys.*, 1982, **77**, 3654–3665; P. C. Hariharan and J. A. Pople, *Theor. Chim. Acta*, 1973, **28**, 213–222; W. J. Hehre, R. Ditchfield and J. A. Pople, *J. Chem. Phys.*, 1972, **56**, 2257–2261.
- 29 M. J. Frisch, G. W. Trucks, H. B. Schlegel, G. E. Scuseria, M. A. Robb, J. R. Cheeseman, J. A. Montgomery Jr., T. Vreven, K. N. Kudin, J. C. Burant, J. M. Millam, S. S. Iyengar, J. Tomasi, V. Barone, B. Mennucci, M. Cossi, G. Scalmani, N. Rega, G. A. Petersson, H. Nakatsuji, M. Hada, M. Ehara, K. Toyota, R. Fukuda, J. Hasegawa, M. Ishida, T. Nakajima, Y. Honda, O. Kitao, H. Nakai, M. Klene, X. Li, J. E. Knox, H. P. Hratchian, J. B. Cross, V. Bakken, C. Adamo, J. Jaramillo, R. Gomperts, R. E. Stratmann, O. Yazyev, A. J. Austin, R. Cammi, C. Pomelli, J. W. Ochterski, P. Y. Ayala, K. Morokuma, G. A. Voth, P. Salvador, J. J. Dannenberg, V. G. Zakrzewski, S. Dapprich, A. D. Daniels, M. C. Strain, O. Farkas, D. K. Malick, A. D. Rabuck, K. Raghavachari, J. B. Foresman, J. V. Ortiz, Q. Cui, A. G. Baboul, S. Clifford, J. Cioslowski, B. B. Stefanov, G. Liu, A. Liashenko, P. Piskorz, I. Komaromi, R. L. Martin, D. J. Fox, T. Keith, M. A. Al-Laham, C. Y. Peng, A. Nanayakkara, M. Challacombe, P. M. W. Gill, B. Johnson, W. Chen, M. W. Wong, C. Gonzalez and J. A. Pople, *GAUSSIAN 09 (Revision A.02)*, Gaussian, Inc., Wallingford CT, 2009.